Development of outdoor luminescence imaging for drone-based PV array inspection

Benatto, Gisele Alves dos Reis; Riedel, Nicholas; Thorsteinsson, Sune; Poulsen, Peter; Thorseth, Anders; Dam-Hansen, Carsten; Mantel, Claire; Forchhammer, Søren; H. B. Frederiksen, Kenn; Vedde, Jan; Petersen, Michael; Voss, Henrik; Messerschmidt, Michael; Parikh, Harsh; Spataru, Sergiu; Sera, Dezso

Published in:
Proceedings of the 44th IEEE Photovoltaic Specialists Conference, PVSC 2017

DOI (link to publication from Publisher):
10.1109/PVSC.2017.8366602

Publication date:
2017

Document Version
Accepted author manuscript, peer reviewed version

Development of outdoor luminescence imaging for drone-based PV array inspection

Gisele A. dos Reis Benatto[1], Nicholas Riedel[1], Sune Thorsteinsson[1], Peter B. Poulsen[1], Anders Thorseth[1], Carsten Dam-Hansen[1], Claire Mantel[1], Søren Forchhammer[1], Kenn H. B. Frederiksen[2], Jan Vedde[3], Michael Petersen[4], Henrik Voss[5], Michael Messerschmidt[5], Harsh Parikh[6], Sergiu Spataru[6] and Dezso Sera[6]

[1]Department of Photonics Engineering, Technical University of Denmark, Frederiksborgvej 399, 4000, Roskilde, Denmark
[2]Kenergy, Grønningen 43, 8700, Horsens, Denmark
[3]SiCon Silicon & PV consulting, J N Vinthersvej 5, 3460, Birkerød, Denmark
[4]Skive Kommune, Torvegade 10, 7800 Skive, Denmark
[5]Sky-Watch A/S, Østre Alle 6 Støvring, Nordjylland, 9530, Denmark
[6]Aalborg University, Aalborg, 9220, Denmark

***Abstract* — In this work we investigate and present preliminary results for two methods for luminescence imaging of photovoltaic (PV) modules in outdoor conditions, with the aim of choosing the most suitable method for implementation on a drone PV plant inspection system. We examined experimentally both electroluminescence (EL) and photoluminescence (PL) PV module imaging methods under natural light conditions, and determined that fast pulsed EL imaging with InGaAs detector cameras can yield reasonably accurate results under daylight conditions. Moreover, we formulated the necessary requirement for a PL light source, which would allow PL imaging of modules under daylight conditions.**

***Index Terms* — drone-based PV inspection, electroluminescence imaging, image processing, outdoor defect detection, photoluminescence imaging.**

I. Introduction

In order to ensure expected return on investment (ROI) of small and large-scale photovoltaic (PV) installations, regular fault detection for effective maintenance, is highly important. Present day PV panels are designed to operate for 25-30 years, however field experience shows that after 11-12 years of operation 2% or more of all PV panels fail [1]. However, the failure rate is even higher for older installations, especially those manufactured before the year 2000 [2].

In practice, the frequency and inspection detail level is often limited by manpower and cost. Presently, drone-based infrared (IR) thermography inspection of solar plants is a reality, and the technology is expected to develop further into automated solar plant inspection [3]–[5]. The accuracy of thermographic fault detection though, presents limitations – primarily related to deconvoluting the failure signature into failure type and severity, which can be overcome when performed in combination to electro-(EL) or photo-(PL) luminescence imaging of the panels. The combination of defect detection techniques has been already tested in laboratory [1], [6], although many limitations still need to be addressed in order to obtain image acquisition outdoors and integrate, automatize and optimize the imaging system in a drone.

In this work, we investigate and present preliminary results for two methods for luminescence imaging of PV modules in outdoor conditions, with the aim of choosing the most suitable method for implementation on a drone PV plant luminescence inspection system. First, we investigate a pulsed EL imaging method under daylight conditions, to determine the necessary camera and measurement parameters. In the second part, we examine a PL imaging method under natural low light conditions, do determine if PL imaging would be feasible for outdoor PL imaging, along with the necessary light source requirements. The concept of PL/EL in a drone is illustrated in Fig. 1.

Fig. 1. Sketch of the concept of automatized drone inspection.

II. Experiment and Methodology

The experimental tests performed in this work are focused on investigating EL and PL imaging techniques that are suitable for implementation into a drone-based inspection system. The PL technique avoids the need for electrical contact into the solar panels, which is a time limiting factor for drone-based inspection, especially in large-scale solar plants.

The luminescence emission peak for silicon-based solar cells at ambient temperature is at 1150 nm [7], near a water absorption band in the solar spectrum (AM 1.5), as illustrated in Fig. 2. In the same figure, the quantum efficiencies of two camera detectors: i) a cooled Si charge-coupled device (CCD) ii) and short-wave infrared (SWIR) InGaAs, able to detect the emission peak, are plotted. Comparing the curves with the peak positions it is clear that a CCD camera can acquire only a small portion of the emission peak. At the same time, the SWIR InGaAs can detect the emission entirely, providing fast integration times, ideal for drone operation. Additionally, the InGaAs detector avoids the most intense section of the solar spectrum. Even though, to avoid the relatively intense sunlight, a sharp optical band-pass filter is used, with the transmission wavelength illustrated as the white area in Fig. 2.

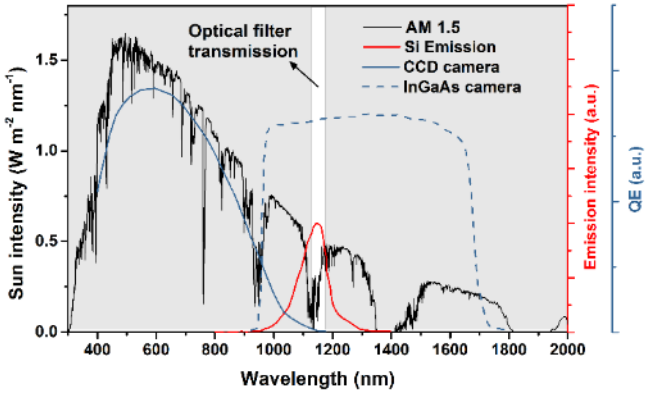

Fig. 2. AM 1.5 sun spectrum (black line), CCD (solid blue line) and InGaAs (dashed blue line) camera QE curves, and silicon emission peak (red line). The grey areas show wavelengths that are cut off with the use of an optical filter in order to avoid detection of the sunlight.

A. Electroluminescence

The EL images shown in this paper are acquired from a mechanically stressed 36 cell multicrystalline silicon solar panel with 1 x 1 meter dimension. An InGaAs camera from Hamamatsu model C12741-03, and an OD>4.0 1150nm band-pass filter with 50nm FWHM was used to obtain all EL images.

A sequential image acquisition system was implemented in order to enhance the quality of the images obtained at high noise level during the day. Such system synchronizes the image acquisition with an electrical forward bias applied by a DC power supply. Fig. 3 illustrates the synchronizing circuit, driven by an Arduino logic controller, and the pulse width modulated (PWM) waveforms applied to the PV panel and camera. The exposure time is established separately in the camera software.

To estimate the effect of the sun on the imaging process and to better understand the noise characteristics towards an InGaAs detector and develop image processing strategies, we acquired sequences of 100 images (50 under forward bias (signal) and 50 as background images for subtraction) at 6 Hz with 20 ms exposure time, under 300, 500, 600, and 800 W/m^2

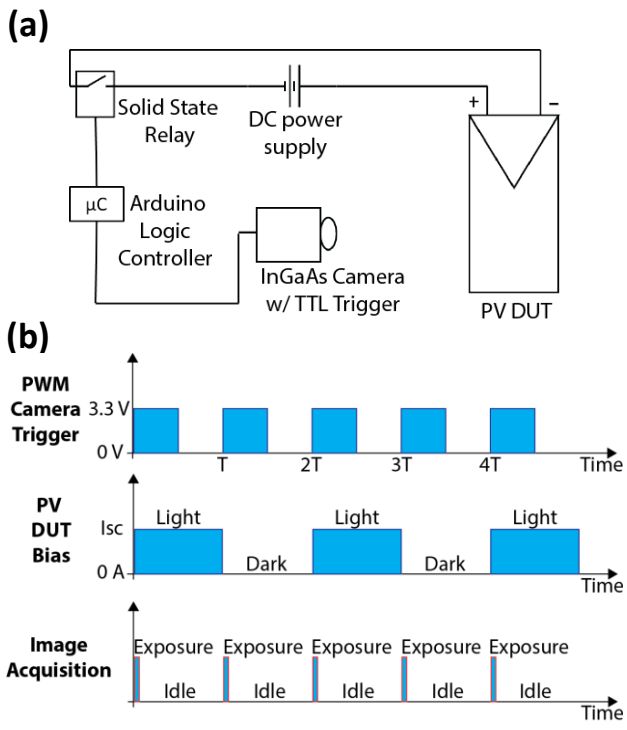

Fig. 3. Basic trigger circuit that synchronizes the imaging and forward bias from a DC power supply (a); and the PWM waveforms driven by the Arduino logic controller (b).

global horizontal irradiance (GHI). The solar irradiance was acquired by a weather station [8] located just few meters from the imaging position. The iris aperture was f4 for 300 W/m^2 and f8 for the remaining. The images were acquired at around 2.6 meters from the panel.

As averaging several pictures is the most common way the minimize noise from images, we perform it the enhance image quality. The image processing included taking the difference between the average of light and dark images, automatic stretching of the initial dynamic range (the source images are 16bits) to 8 bits for display and cropping of the whole image to the region of interest. T-tests of the images pixel values were performed for better understanding of signal the noise ratio (SNR).

B. Photoluminescence

PL images indoors were acquired using a laser diode at 800 nm with capacity of 13 W maximum optical power, while the camera and the laser were circa 0.5 meter far from the sample. The sample consisted of a multicrystalline silicon cracked PV cell. The same camera and filter used for EL was used to obtain PL images. The images were acquired at 700 ms exposure time for 54, 71, 87, 104 and 120 W/m^2 light intensity on the plan of the cell, which corresponded respectively to 3, 4, 5, 6 and 7 W of optical power from the laser.

III. Results and Discussion

A. Electroluminescence

EL imaging during the night is comparable to indoors EL imaging, where normally there is no significant ambient light noise levels. For comparison, Fig. 4 shows the indoors EL image of the mechanically stressed module. However, during the day such images are surrounded by high, and very often variable, light noise levels, primarily from the sunlight itself.

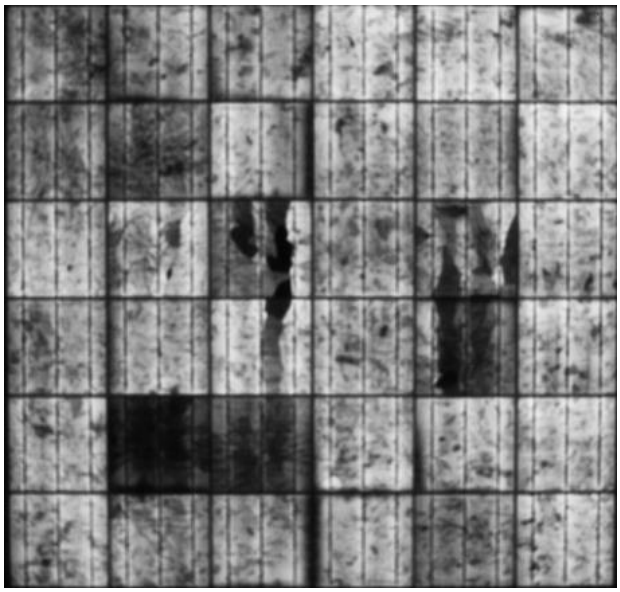

Fig. 4. Indoors EL image of mechanically stressed PV module, showing cracks and disconnected cell areas.

Fig 5a shows the EL images acquired under different sun irradiation levels, after averaging, subtracting, and image processing. The irradiance on the plane of the module array (POA) was 117.6, 332.3, 467.8, and 714.5 W/m^2 respectively; using the Hay Davie's model for diffuse irradiance on a tilted surface [9]. At 800 W/m^2 for example, there was a strong direct beam irradiance when the image was taken, which did not limit the EL image quality after processing. All the final images present roughly similar information for broken cells and shunt defects present in the module and detected in Fig. 4.

The plots in Fig. 5b show the two sample t-tests that compare the image pixel values under dark (0 current bias) and light (I_{SC} bias) conditions for each test irradiance. The y-axis show the summation of pixel values in the InGaAs detector (512x640), where the value of each pixel is a value between 0.0 (i.e. completely dark) and 1.0 (i.e. completely saturated).

Each t-test shows data from 50 light and 50 dark images at a given irradiance. The green diamonds show the 95% confidence interval of the mean wherein the horizontal green line shows the mean and the top and bottom corners show the confidence interval. The dark and light pixel distributions are considered significantly different when the confidence intervals do not overlap. The t-tests show that the dark and light pixel distributions are significantly different ($p < 0.05$) for all irradiances except for 500 W/m^2 ($p = 0.06$). The difference between dark (background) and light (I_{SC} bias) image means illustrates how it was possible to obtain the images in Fig. 5a. As the difference decreases with the irradiation level, the SNR was lower, yet with significant difference.

The sun intensity though constantly varies during the image acquisition, dependent on to the time of the day and cloud cover. Fig. 5c show the time series of light and dark images sequences, as their pixel values changed during the circa 17 seconds that sequence took to acquire. Such variation is directly related to the ambient illumination (sun intensity) variation as it equally affects both the light and background reference (dark) images. Even though irradiance fluctuations bring challenges in particular situations, such variations did not impose visual limitations in the daylight outdoor EL imaging after processing. Nevertheless, automatic aperture adjustment will be required to avoid image saturation during drone inspection.

Averaging several pictures is the most common way the minimize noise from images. Although, to take several pictures of the same scene, if the system camera-power supply is not fast enough, it can be limiting for the drone movement. Fig. 6 shows the resulting averaged and subtracted images when different amounts of light and dark images are used under. All images in Fig. 6 were taken under 300 W/m^2 illumination in natural sunlight. The average of 8 light and dark images (16 in total images), show a good level of noise removal. For this, it is required that the drone keeps position for 0.32s, with a power supply as fast as the camera triggering for 20ms exposure time. This is achievable if the drone is equipped with an appropriate camera stabilization gimbal, in addition to performing digital imaging stabilization on the acquired images. However, fewer averaged pictures does allow the detection of major defects in this example.

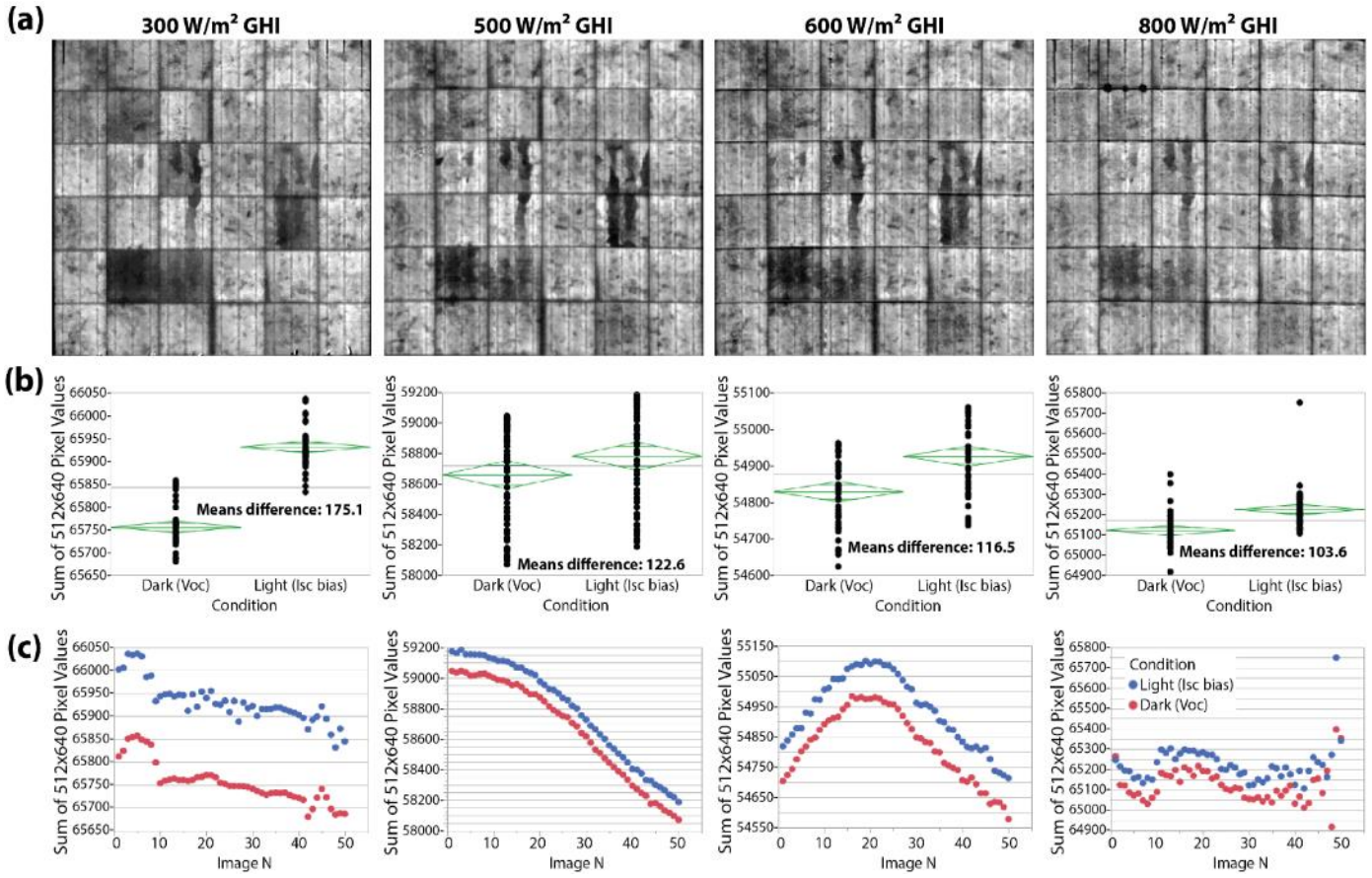

Fig. 5. EL images obtained under different sun irradiation levels, after image processing, automatic cropping and contrast correction (a); sum of pixel values of dark and light images of the correspondent image above, with the mean and 95% confidence interval shown as green diamonds (b); correspondent time series of light (blue dots) and dark (red dots) images, showing variations of light intensity during the acquisition of the sequence of images (c).

B. Photoluminescence

In addition to the outdoors EL imaging tests, laboratory PL tests were performed. Fig. 7 show the images acquired at 700 ms exposure time for 54, 71, 87, 104 and 120 W/m^2 light intensity on the plan of the cell. Therefore, long exposure times were required for such low illumination rates. As the intensity of a light source complies with the inverse-square law, even a powerful light source will have limited maximum distance from the panels. At the same time, such powerful light source will require cooling, which poses size and weight challenges for the drone.

For the development of the best strategy of minimum weight and best light source for PL outdoor imaging, a measurement modeling was developed, in order to correlate the relevant variables of the system. Such model for the PL image signal generated by an artificial light source (S) in arbitrary units can be expressed as the equation below:

$$S = \frac{1}{D^2}\,\frac{P_{optical}}{A}\,\tau\,\eta_{PL}(\lambda_{Light})\,\rho_{Camera}(\lambda_{PL}) \qquad (1)$$

Where D is the distance from sample (panel) to the light source; $P_{optical}$ is the optical power output of the light source which is related to the electrical power input and device

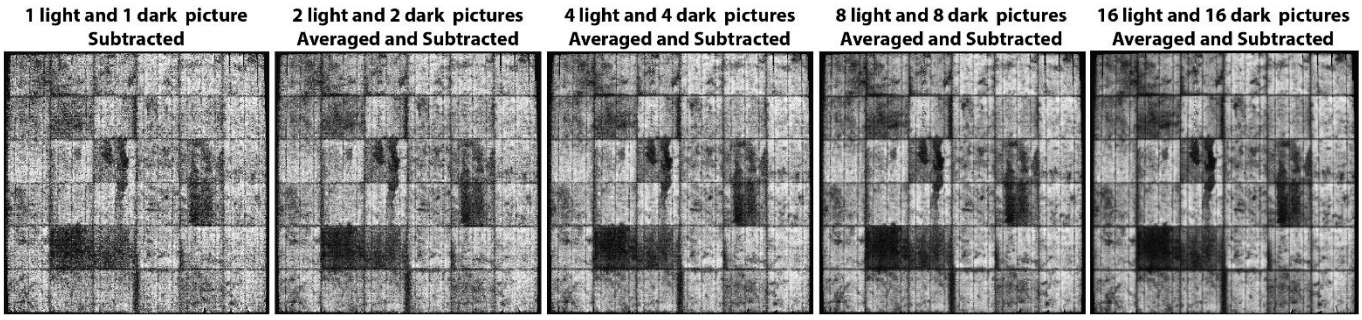

Fig. 6. Averaged and subtracted EL pictures of a solar panel acquired outdoors under 300 W/m^2 sun illumination.

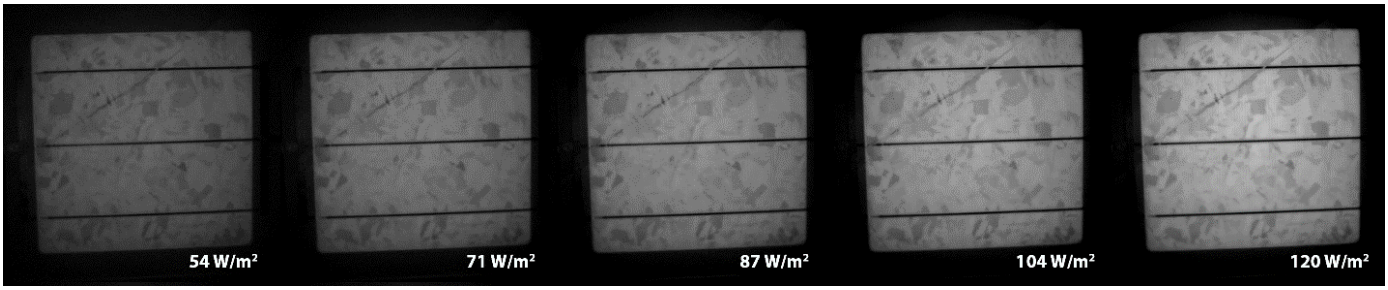

Fig. 7. PL images taken using 800nm laser diode, under 700ms exposure time, from a polycrystalline silicon wafer under different illumination.

efficiency, leading to known heating and consequentially the need for certain cooling. A is the area to be illuminated, contained by designed optics in order to avoid light loss. τ is the exposure time or the time required for the light to be on, here correspondent also to the camera exposure time. $\eta_{PL}(\lambda_{Light})$ is the PL quantum yield, related to the absorbed photons in the PV module (PV/silicon quantum efficiency) at the given wavelength of the light source and reemitted in the same direction as the incident light. $\rho_{Camera}(\lambda_{PL})$ is the camera acquisition factor that correlates quantum efficiency, dynamic range, among other sensor and camera designed features, at a certain wavelength, in this case correspondent to the luminescence signal wavelength (centred at 1150 nm).

With such vision of the system, it was possible to correlate the signal response measured in the laboratory with the needed requirements to build a drone integrated light source that will allow outdoor PL imaging. Taking into consideration the available technologies, a laser line scan following the drone movement is the one that complies sufficiently with optical power and current image acquisition requirements. In this case, the area needed to be illuminated is smaller, making the $\frac{P_{optical}}{A}$ factor lower. Fig. 8 illustrates the above described approach.

According to (1), the laser line scan approach with current available technology will able to acquire the similar signal presented in Fig. 7 (71 W/m^2) at three meters distance of a full size module with 20 ms exposure time. Another example would

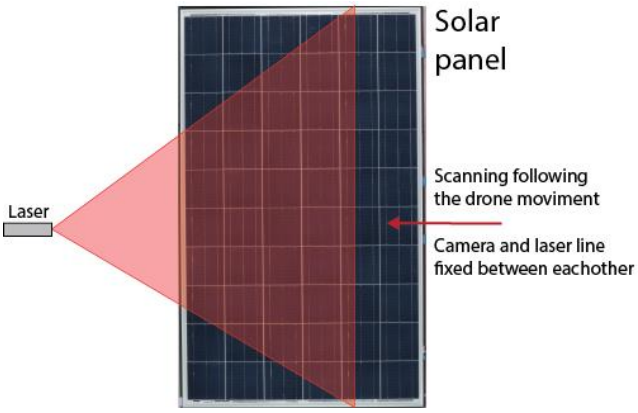

Fig. 8. Laser line scan PL approach.

be a fast pulsing high power laser, supplied by capacitors. The approaches as pulsing laser and LEDs so far presented too low signal intensity for the current setup, but as the whole system is in development, they are not discarded.

V. Conclusion

The EL imaging performed for PV inspection during the day under high sun intensity address the possibility of performing EL imaging inspection with more freedom, during more hours of the day, and simultaneous IR and EL. In a drone system, the compatibility will remain the same for either daylight or nighttime EL. In future work the forward bias and camera triggering will be carried out via wireless communication. In addition, we will focus efforts on improving imaging processing, which can be done automatically and without losing flight time.

The next step for this analysis is to develop a controllable test bed with a moving camera and check the limit of frames from a video taken at certain speeds. The camera used in this work has the maximum frame rate of 60 fps, which is relatively low for this application. Consequently, a faster camera will allow more pictures to be taken in a shorter period, and the future tests will define how fast the drone can move while it takes different amounts of pictures for the image processing.

The PL indoor measurement parameters permitted the measurement modeling for the light source development, which indicates a line laser scan as the most promising light source for outdoor PL and drone integration.

Acknowledgement

The authors acknowledge the financial support from Innovation Fund Denmark for the project 6154-00012B DronEL – Fast and accurate inspection of large photovoltaic plants using aerial drone imaging.

References

[1] M. Köntges *et al.*, “Review of Failures of Photovoltaic Modules,” 2014.

[2] D. C. Jordan and S. R. Kurtz, “Photovoltaic degradation rates - An Analytical Review,” *Prog. Photovoltaics Res. Appl.*, vol.

21, no. 1, pp. 12–29, 2013.

[3] S. Dotenco *et al.*, "Automatic detection and analysis of photovoltaic modules in aerial infrared imagery," *2016 IEEE Winter Conf. Appl. Comput. Vis.*, pp. 1–9, 2016.

[4] "The drones that inspect and maintain photovoltaic power plants," *sUAS News - The Business of Drones*. [Online]. Available: https://www.suasnews.com/2015/04/the-drones-that-inspect-and-maintain-photovoltaic-power-plants/. [Accessed: 25-Jan-2017].

[5] "Drones to cut plant inspection costs as South Africa eyes quality," *PV Insider*. [Online]. Available: http://analysis.pv-insider.com/drones-cut-plant-inspection-costs-south-africa-eyes-quality. [Accessed: 25-Jan-2017].

[6] S. Johnston and T. Silverman, "Photoluminescence and Electroluminescence Imaging Workstation," *NREL*, 2015.

[7] W. S. Yoo, K. Kang, G. Murai, and M. Yoshimoto, "Temperature Dependence of Photoluminescence Spectra from Crystalline Silicon," *ECS J. Solid State Sci. Technol.*, vol. 4, no. 12, pp. P456–P461, 2015.

[8] DTU Fotonik, "DTU Risø PV Weather Data." [Online]. Available: http://ftnk-psolmaal.win.dtu.dk/B130_PV_Weather/index.html. [Accessed: 18-May-2017].

[9] J. E. Hay and J. A. Davies, "Calculations of the solar radiation incident on an inclined surface," in *Proc. of First Canadian Solar Radiation Data Workshop*, 1980, p. 59.